Transient formation of water-conducting states in membrane transporters

Jing Li, Saher A. Shaikh, Giray Enkavi, Po-Chao Wen, Zhijian Huang, and Emad Tajkhorshid[1]

Center for Biophysics and Computational Biology, Department of Biochemistry, and Beckman Institute for Advanced Science and Technology, University of Illinois at Urbana–Champaign, Urbana, IL 61801

Edited by Michael L. Klein, Temple University, Philadelphia, PA, and approved March 27, 2013 (received for review October 31, 2012)

Membrane transporters rely on highly coordinated structural transitions between major conformational states for their function, to prevent simultaneous access of the substrate binding site to both sides of the membrane—a mode of operation known as the alternating access model. Although this mechanism successfully accounts for the efficient exchange of the primary substrate across the membrane, accruing evidence on significant water transport and even uncoupled ion transport mediated by transporters has challenged the concept of perfect mechanical coupling and coordination of the gating mechanism in transporters, which might be expected from the alternating access model. Here, we present a large set of extended equilibrium molecular dynamics simulations performed on several classes of membrane transporters in different conformational states, to test the presence of the phenomenon in diverse transporter classes and to investigate the underlying molecular mechanism of water transport through membrane transporters. The simulations reveal spontaneous formation of transient water-conducting (channel-like) states allowing passive water diffusion through the lumen of the transporters. These channel-like states are permeable to water but occluded to substrate, thereby not hindering the uphill transport of the primary substrate, i.e., the alternating access model remains applicable to the substrate. The rise of such water-conducting states during the large-scale structural transitions of the transporter protein is indicative of imperfections in the coordinated closing and opening motions of the cytoplasmic and extracellular gates. We propose that the observed water-conducting states likely represent a universal phenomenon in membrane transporters, which is consistent with their reliance on large-scale motion for function.

major facilitator superfamily | LeuT-fold transporters | ABC transporters | neurotransmitter transporters

Membrane transporters provide efficient mechanisms for exchange of diverse molecular species across the cellular membrane generally in an active manner. By coupling various forms of chemical energy in the cell to a set of highly coordinated conformational transitions, membrane transporters fuel vectorial translocation of their respective substrates across the membrane. From a structural perspective, the overall process of transport is furnished through transitions between two major conformational states—namely, the outward-facing (OF) and inward-facing (IF) states (1)—during which substrate accessibility is shifted from one side of the membrane to the other. Central to efficient transport and to preventing dissipation of the substrate down the electrochemical gradient is to ensure that the substrate binding site will not be accessible simultaneously to both sides of the membrane, a mechanism best known as the alternating access model (2). This model, which has received substantial support from biochemical, kinetic, and structural studies (1, 3, 4), relies on a high level of coordination between two gating mechanisms, a cytoplasmic and an extracellular one, exposing the substrate binding site to only one side of the membrane at a time. This key mechanistic aspect defines the main distinction of transporters from membrane channels, in which opening of a single gate usually creates the transmembrane substrate permeation pathway to connect both sides of the membrane simultaneously (5).

Interestingly, various experimental studies have reported water transport and uncoupled ion transport for several membrane transporters (6–8), a phenomenon that might appear to contradict the traditional understanding of the alternating access model. Water exchange mediated by membrane transporters has been attributed to two fundamentally different mechanisms: passive, osmosis-driven water exchange (9) and active, stoichiometrically related cotransport of water (6). Though the involvement of osmosis-driven mechanism has been well established (9), the role of active water cotransport is still a subject of debate, and various models have been proposed to account for it (6). These models include the carrier-mediated model, which relies on the uptake of a large number of water molecules along with the substrate into the binding region/lumen of the transporter and their simultaneous pumping to the other side of the membrane (10–12), and cotransport of water as a result of osmotic imbalance introduced by the local accumulation of the nonaqueous substrate (13–15).

A detailed investigation of the mechanism(s) for transporter-mediated water exchange across the membrane requires not only high-resolution structures of membrane transporters, but also a dynamical description of the protein and transported species. Recent years have witnessed a sharp increase in the number of crystal structures of membrane transporters in different conformational states, thereby providing valuable insight into their mechanisms (3, 4). Though several of these structures are reported at resolutions high enough to gain information on the position of a few water molecules, none seems to offer a convincing mechanism for water transport. Thus, it appears necessary to examine the dynamics of the protein as well as water to gain insight into the mechanistic details of the process. In this context, molecular dynamics (MD) offers a powerful tool to capture conformational fluctuations of the transporter, which are closely coupled to formation of water permeation pathways, and to describe the dynamics of smaller species, such as water, substrate, and ions during the structural breathing of the protein (16).

In this study, we used MD simulations to study a diverse set of membrane transporters (Table 1) with the primary goal of characterizing the mechanism of water transport. Extended equilibrium simulations of membrane-embedded structures are performed for transporters from the solute sodium symporter (SSS), solute carrier 1 (SLC1), major facilitator superfamily (MFS), nucleobase-cation-symport-1 (NCS1), and ATP binding cassette (ABC) families/superfamilies—namely, Na^+-coupled glucose transporter (vSGLT), glutamate transporter (GlT), glycerol-3-phosphate transporter (GlpT), benzyl hydantoin transporter (Mhp1), and maltose transporter, respectively. We note that for some of the transporter families studied here, the phenomenon of water transport has not yet been reported experimentally. We observe the formation of

Author contributions: J.L., S.A.S., and E.T. designed research; J.L., S.A.S., G.E., P.-C.W., and Z.H. performed research; J.L., S.A.S., G.E., P.-C.W., and Z.H. analyzed data; and J.L., S.A.S., G.E., P.-C.W., Z.H., and E.T. wrote the paper.

The authors declare no conflict of interest.

This article is a PNAS Direct Submission.

Freely available online through the PNAS open access option.

[1]To whom correspondence should be addressed. E-mail: emad@life.illinois.edu.

This article contains supporting information online at www.pnas.org/lookup/suppl/doi:10.1073/pnas.1218986110/-/DCSupplemental.

Table 1. Simulated systems

Transporter	Substrate/ion	Family or superfamily	State	Simulation time
vSGLT	Na^+/glucose	SSS	IF substrate-bound	1.15 μs
Glt_{ph}	Na^+/glutamate	SLC1	intermediate apo	160 ns
GlpT	Glycerol-3-phosphate/P_i	MFS	IF substrate-bound	200 ns
Mhp1	Na^+/benzyl-hydantoin	NCS1	OF substrate-free	1.2 μs
Maltose transporter	Maltose	ABC	OF substrate-bound	100 ns

water-conducting states in all cases, describe their nature and mechanism of formation, and quantify the rate of water transport through these states. To our knowledge, this report provides previously undescribed formation of water-conducting states in multiple transporter families, suggesting that the phenomenon might represent a universal aspect of membrane transporter function.

Results and Discussion

Water-Conducting States of SGLT. The best-documented case of a water-conducting transporter is SGLT, with several studies reporting its characteristic leakiness to small species, such as water, and even ions (9, 11, 13, 17–20). Water transport has also been reported for Na^+-I^- symporter (NIS) (12) and lactate transporter (MCT1) (21), both belonging to the same family (SSS) of transporters as SGLT. More importantly, other leucine transporter (LeuT)-fold transporters have also been reported to exhibit water transport (22, 23). The availability of a crystal structure for the substrate-bound IF state of a bacterial SGLT (vSGLT) (24) provides the opportunity to study the molecular mechanism of water transport in a transporter family and structural topology that are well established experimentally to exhibit the phenomenon.

During a 1.15-μs MD simulation of vSGLT, a large number of water permeation events were detected. On examining the origin and structural basis for water transport, we detected frequent formation of water-conducting states during the simulation (Fig. 1). A clear relationship exists between the degree of the opening of

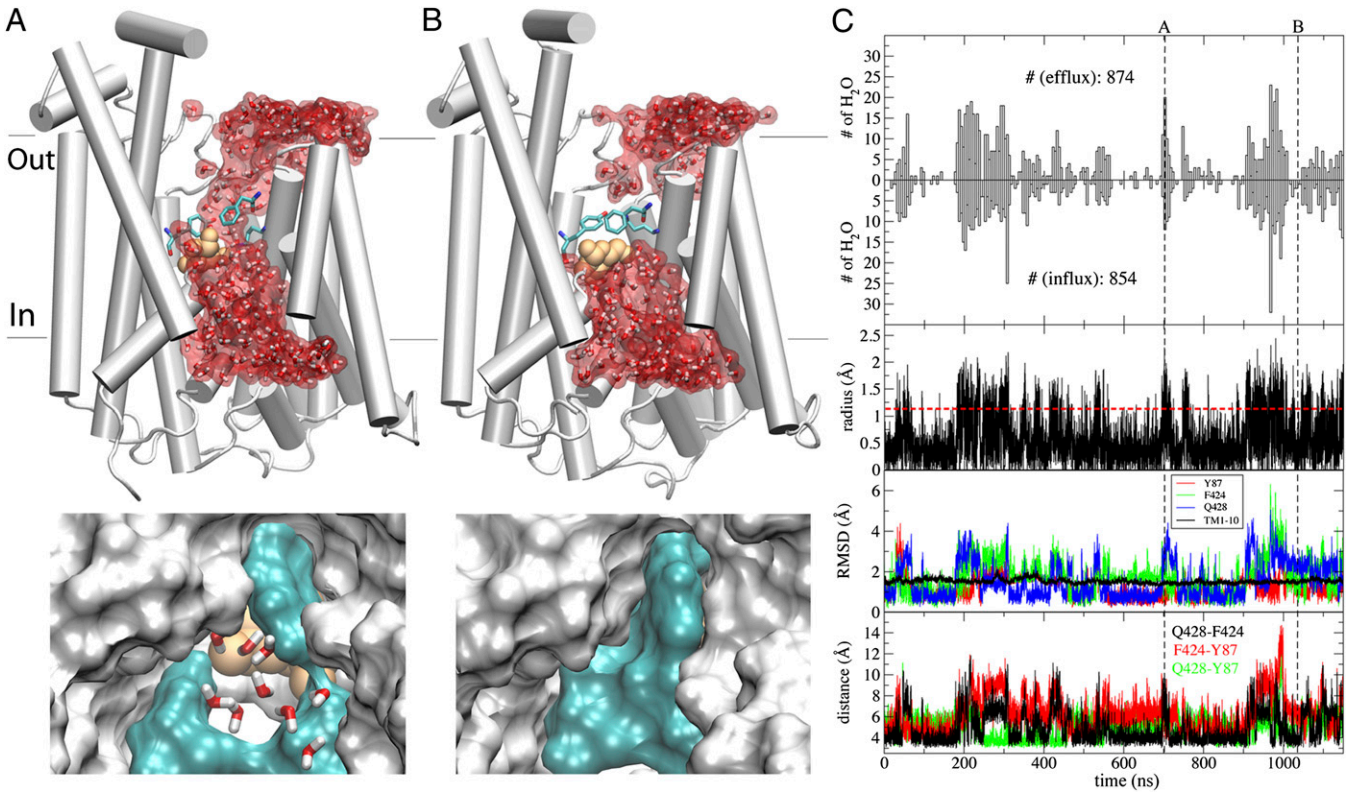

Fig. 1. Water-conducting states and water transport in vSGLT. (*A*) Water-permeable state of vSGLT. (*Upper*) Overall view of the water-conducting state and the continuous water channel formed within the transporter lumen. The protein is drawn in white cartoon, with some of the helices removed for clarity. Water molecules are drawn in both sticks and surface (red) representations, and the substrate in orange van der Waals. The three gating residues controlling water flow— namely, Y87, F424, and Q428—are shown in sticks and colored by atom type. (*Lower*) Close-up view of the same conformation, highlighting the narrowest part of the water permeation pathway. Protein is shown in white surface, except for the three gating residues, which are in cyan surface. (*B*) Water-impermeable conformation of vSGLT. (*Upper* and *Lower*) Same as in *A*, but for a water-impermeable state formed due to side-chain motions of the gating residues (cyan surface) closing the narrowest point along the water permeation pathway. (*C*) Protein dynamics and water transport. The number of observed water permeation events in either direction (influx or efflux) is plotted against the simulation time in the top two panels. The third panel depicts the time series of the minimum radius of the aqueous pathway. The fourth panel shows the rmsd of gating residues and of the core transmembrane domain (10 TMs). The bottom panel shows the time evolution of the distances between the gating residues, i.e., Q428:$N_{\varepsilon 2}$–F424:$C_{\varepsilon 2}$, F424:$C_{\varepsilon 2}$–Y87:$C_{\varepsilon 1}$, and Q428:$N_{\varepsilon 2}$–Y87:$C_{\varepsilon 1}$. The vertical black dashed lines in *C* mark the snapshots shown in *A* and *B*, respectively, and the horizontal red dashed line is used to indicate the minimum radius needed to accommodate a water molecule.

the water-conducting state at its narrowest point (the "constriction point"), and the number of permeating water molecules (Fig. 1*C*).

The water-conducting states are transient in nature, forming and disappearing frequently, thereby resulting in the fluctuation of the number of permeating water molecules (Fig. 1). The aqueous pathway in these states coincides with the putative substrate translocation pathway. This observation is in agreement with experimentally measured inhibitory action of phlorizin, a competitive inhibitor of substrate transport, on water flux, suggesting that these may share the same pathway (9). Remarkably, the radius of the constriction point of the water pore formed within the lumen never reaches above 2.5 Å, which is larger than the radius of water (~1.15 Å) but smaller than that of the primary substrate (~4.0 Å), thus preventing it from leaking back down its chemical gradient.

During the simulation, the protein maintains its IF state as in the crystal structure; this is indicated by the low structural deviation (rmsd < 2 Å) during the simulation (Fig. 1*C*) for the 10 transmembrane (TM) helices. Meanwhile, structural deviation of side chains lining the constriction point, namely Y87, F424, and Q428, and the resulting change in their distances, show a high correlation with the water transport (Fig. 1*C*). Y87 and F424 have been proposed to form the extracellular gate (24), and Q428 has been implicated in direct substrate binding (24). Therefore, in addition to their role in controlling substrate access, these three residues appear to also act as the "gate" for water transport in the IF state of SGLT. The formation of the water-conducting states, in SGLT, therefore, is mainly a result of local conformational changes of a few side chains of these gating residues.

The osmotic permeability (P_f) of vSGLT estimated from these simulations is 4.75×10^{-15} cm^3/s, which is an order of magnitude higher than the experimentally measured value of 4.5×10^{-16} cm^3/s for rSGLT (25). It may be noted here that the P_f values obtained from these simulations are only based on a partial view of the complete transport cycle, i.e., only the IF substrate-bound state, and therefore do not reproduce the average permeability of the complete cycle, reflected in the experimental P_f value. It is expected that increased sampling of more states would bring experiment and simulation results closer to each other. The larger gap between the P_f values for vSGLT calculated from a shorter simulation (200 ns) (19) and the experimental value is in line with this notion.

Water-Conducting States in Other Transporter Families. Examining the dynamics of water in other transporter systems, we were surprised to find that the formation of water-conducting states is not unique to vSGLT. In fact, we observed water transport in four other transporter systems, namely, Glt_{ph}, GlpT, Mhp1, and maltose transporter (Figs. 2 and 3). Unlike vSGLT, water-conducting states in these transporters appear to be associated with the transition of the transporters from one major functional state to another, due either to the intermediate nature of the initial crystal structure or to large structural changes induced during the simulations by mechanistically relevant molecular events as described below (and detailed in *SI Text*).

GlTs [also termed excitatory amino acid transporters (EAATs)] belong to the SLC1 family of neurotransmitter transporters, which are responsible for the clearance of neurotransmitters from the synapse after their release from the presynaptic neurons. Several states of a bacterial GlT homolog (Glt_{ph}) have been structurally resolved, i.e., the OF (26), IF (27), and intermediate (28) states. GlT is an experimentally well-documented case of a transporter mediating water exchange across the membrane during its function, and both osmosis-driven and cotransport mechanisms have been proposed for it (29–31).

Using the trimeric structure of Glt_{ph} (28) with one monomer in the intermediate state (and the other two monomers in the IF state), we have performed a 160-ns MD simulation of the apo (substrate/ion-free) state. These simulations have been performed under the exact same conditions used previously in our laboratory to simulate the OF and IF states of Glt_{ph} (32, 33). During the simulation, numerous water permeation events occur along a continuous aqueous pathway formed at the interface between the transport domain [specifically, helical hairpin 1 (HP1)] and the trimerization domain, but only in the monomer, which is in the intermediate state (Fig. 2). The characterized pathway and mechanism are consistent with a proposed mechanism for water transport in a human GlT (31) and the crystal structure of Glt_{ph} in the intermediate state (28), suggesting that water transport through GlT is mediated via a putative Cl^- leak pathway of the transporter. The radius of the constriction point in the intermediate Glt_{ph} (~1.5 Å) remains always smaller than that of the substrate (Fig. 2). Although the intermediate nature of this monomer well accounts for the most part of the water permeation pathway, further conformational fluctuation of HP1 seems to be necessary for the formation of the full water channel (see *SI Text* for details). No water exchange was observed in the other two monomers, or in our previous simulations performed on trimeric

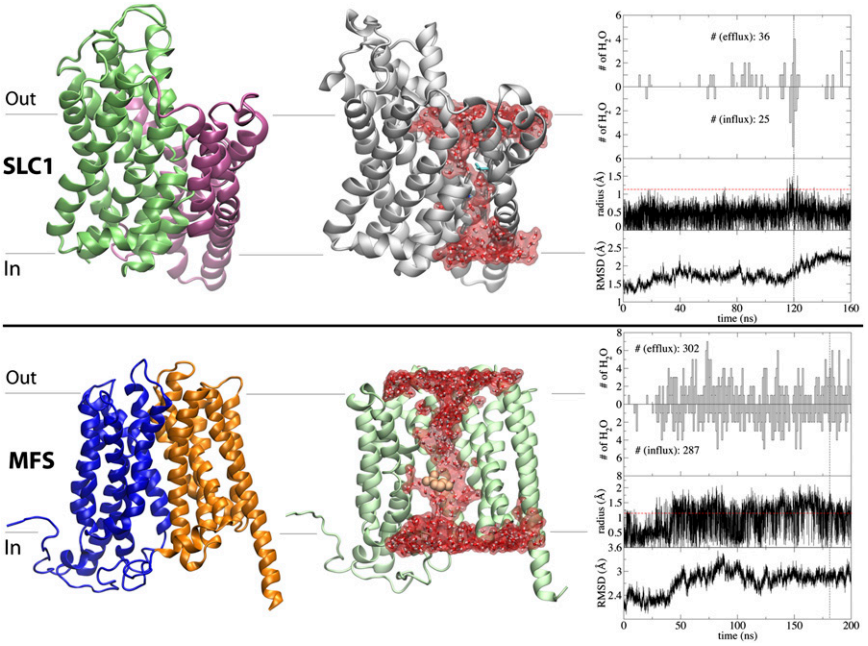

Fig. 2. Water-conducting states for Glt_{ph} (EAAT) of the SLC1 family (*Upper*) and GlpT from the MFS superfamily (*Lower*). (*Left*) Topology of the protein using the crystal structure, highlighting in different colors functionally relevant domains and repeats. Though Glt_{ph} is simulated as a trimer, here only the monomer in the intermediate state is depicted, with the transport and trimerization domains colored in green and purple, respectively. (*Center*) Representative water-conducting frame from the simulations. (*Right*) Time series for the number of water permeation events along the efflux and influx directions, radius of the narrowest part along of the aqueous lumen, and C_α rmsd of the TM region. The vertical black dashed lines represent the snapshots shown in the molecular images, and the horizontal red dashed lines show the minimal radius to accommodate a water molecule.

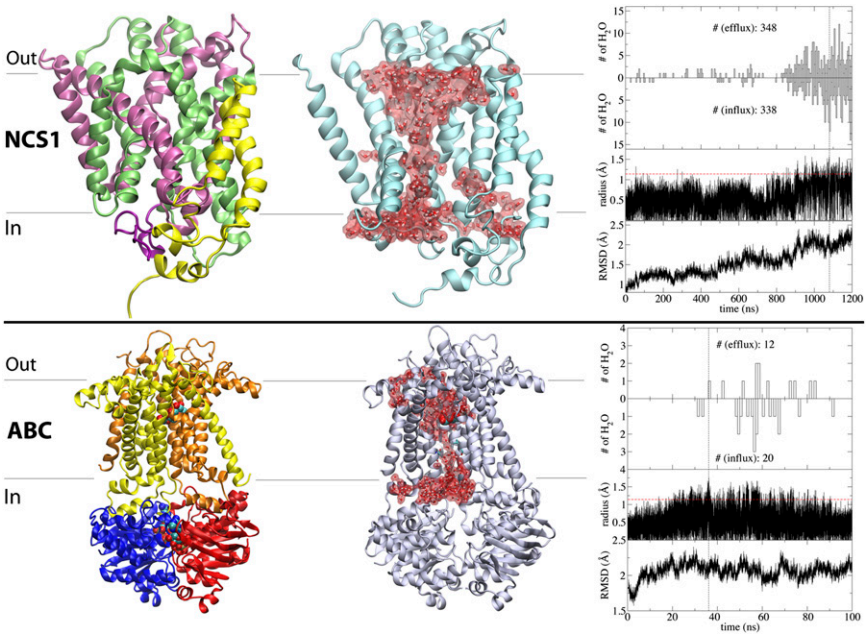

Fig. 3. Water-conducting states for Mhp1 of the NCS1 family (*Upper*) and maltose transporter of the ABC superfamily (*Lower*). The panels are arranged in the same manner as in Fig. 2. (*Left*) crystal structure. (*Center*) Representative water-conducting state. (*Right*) Time series for key events. For clarity here, only the TM domains and NBDs are depicted in maltose transporter.

states of either OF or IF states in numerous different bound states. Together, these results strongly associate the observation of the water-conducting state with the intermediate character of Glt_{ph}.

The third studied membrane transporter is GlpT, one of the few structurally known members of the MFS superfamily, the largest superfamily of secondary active transporters (34). Although no study implicating GlpT in water transport currently exists, other MFS transporters, most prominently glucose transporters GLUT1 and GLUT2, have been reported to exhibit water transport (35, 36).

During a 200-ns simulation of substrate-bound, IF-state GlpT (37, 38), we observed copious water transport events (Fig. 2). Similar to vSGLT, water permeation in GlpT occurs via an aqueous pathway running through the substrate binding site, and the radius of the constriction point remains smaller than that of the main substrate (Fig. 2). However, the scale of conformational changes preceding the formation of the water-conducting state differs from vSGLT. It is important to note that water permeation in GlpT was only observed following two functionally relevant events—namely, substrate binding, which happened spontaneously in equilibrium simulations (37, 38), and a subsequent proton transfer reaction, which was modeled by the change of the protonation state of a conserved histidine in the binding pocket. These molecular events are deemed to be necessary for triggering/facilitating large-scale structural transitions of GlpT from the crystallographically captured state to other major states, the early stages of which seem to have been captured in our simulation (see *SI Text* for more detail). These structural changes include the rearrangements of the two TM domains with respect to each other, resulting in partial opening and closure in the extracellular and cytoplasmic halves, respectively, forming an intermediate state between the OF and IF states, exhibiting water transport. The results offer a putative mechanism of water transport for other MFS members as well, in particular for GLUT1 and GLUT2, where water transport has been demonstrated experimentally (35, 36).

The next transporter studied here, Mhp1, is a Na^+-hydantoin transporter in the NCS1 family, which mediates the uptake of nucleobases and related metabolites (39). Structurally (40, 41), Mhp1 belongs to the LeuT-fold family of transporters. However, though other LeuT-fold transporters, e.g., SGLT1 and LeuT, have been experimentally characterized as water-transporting proteins (17, 22), until now, no water transport has been reported for the NCS1 family.

Transient water-conducting states were observed during a 1.2-μs simulation of the OF state of Mhp1 in its substrate-free form (Fig. 3). As in vSGLT and GlpT, the aqueous pathway overlaps with the putative substrate pathway, whereas the radius of the constriction point (~1.5 Å) is consistently smaller than the substrate (~4.0 Å; Fig. 3), thereby preventing free diffusion of the substrate. Mhp1 is the another transporter discussed here for which the formation of water-conducting states is associated with large-scale structural changes of the protein, in contrast to more localized fluctuations, which seem to be sufficient for the formation of water pores in vSGLT. A significant rearrangement of the cytoplasmic half of the protein appears to accompany the formation of the observed water-conducting state in Mhp1 (Fig. 3). This change is triggered by the spontaneous unbinding of the Na^+ ion from its binding site during the equilibrium simulation (see *SI Text* for details). The presence of the Na^+ ion has been demonstrated experimentally to directly affect the stability of the OF state in LeuT-fold transporters (42, 43).

The last transporter examined for water transport is the *Escherichia coli* maltose transporter (44). Distinct from the secondary transporters described above, maltose transporter is a primary active transporter from the ABC transporter superfamily, with two TM domains forming the substrate translocation pathway (Fig. 3), whose conformational states are determined by ATP binding and hydrolysis within two cytoplasmic nucleotide-binding domains (NBDs; Fig. 3).

Starting from the crystal structure of maltose transporter in the OF state (45), a 100-ns simulation was performed after removing ATP from the two NBDs, as an efficient method to trigger the structural transition toward the IF state (46, 47). The removal of ATP leads to a rapid separation of the NBDs, which in turn translates into the opening of the cytoplasmic ends of the closely coupled TM domains (47). Because the periplasmic end of the transporter is already open in the crystal structure (OF state), the above-described molecular events result in the formation of a water-conducting state through which water permeation events were observed ($t > 30$ ns; Fig. 3). We note that in control simulations performed on the ATP-bound state, no large conformational changes or water permeation events were observed (see *SI Text* for details).

The maximal radius recorded at the constriction point of the aqueous pathway during the simulations is ~1.8 Å, which is sufficiently large to allow water exchange intermittently but not the translocation of the much larger transported substrate (maltose

or maltodextrin). As was the case for most of the transporters studied here, the aqueous pathway in maltose transporter runs through the substrate-binding site (Fig. 3). Herein, we report previously undescribed water transport for a primary active transporter.

Mechanistic Features of Water Transport in Membrane Transporters. The results presented in this study illustrate the presence of a common molecular mechanism of water transport in diverse transporters. Earlier experimental studies on members of SSS, the neurotransmitter sodium symporter (NSS), SLC1, MFS, and other families have detected conduction for water and/or ions (6–9, 22, 30, 35, 36). Together with the results of the present study demonstrating the phenomenon in diverse transporter families, the accumulated evidence on leakiness of membrane transporters suggest that the coordination between opening and closing motions of the two gates in these molecular machines might not be as perfect as generally perceived. Water transport is mediated by well-characterized water-conducting states (pores) that may arise at different steps of the transport cycle, most likely during the transition between major functional states. In all studied cases except one (GlT), the aqueous pathway forms along the putative substrate pathway. The observed formation of a water pore in a different region in Glt_{ph} (between the transport and trimerization domains) is an example highlighting the possibility that such permeation pathways can arise at any mechanically active interface due to various structural defects induced by large-scale transitions of membrane transporters.

In the absence of well-resolved structural and mechanistic descriptions for water and ion leak, the phenomenon might appear initially detrimental to the transporter function, because such leaky states could potentially dissipate substrate gradient across the membrane. Our results, however, clearly demonstrate how such water-conducting states can form frequently in response to different structural fluctuations without interfering with the tight control of the alternating access for the substrate. In all cases, the observed water-conducting states remain impermeable to the main substrate, thereby conforming with the required alternating access model, a principle that only needs to be obeyed by the substrate. Though structural fluctuations of the protein, whether localized gating-like motions or more global transitions, mediate the formation of the water-conducting states, the constriction point within the transporter lumen is found to always remain sufficiently small to prevent the substrate from leaking.

The results presented here provide a structural basis only for a passive (osmosis-driven) mode of water transport, which is also the only mode of water transport consistent with the structures available for membrane transporters. These structures, particularly those captured in an occluded state, e.g., LeuT (48), vSGLT (24), Glt_{ph} (28), and Na+/betaine symporter BetP (49), indicate that the occluded cavity is too small to accommodate more than a few water molecules to be transported along with the substrate in a carrier-mediated fashion. This low capacity differs by an order of magnitude from the number of water molecules transported per turnover in most transporters (6). Nevertheless, because neither our simulations nor the available crystal structures can claim to have fully examined a transport cycle in its entirety, the involvement of an active (carrier-mediated) mode of transport cannot be discarded based on the currently available data. We note that the water-conducting states captured in the simulations can readily account for a high ratio of water/substrate transport. The amount of water transported through these leaky states is simply a function of their lifetime and average water-permeability.

Finally, we note that our simulations do not have any indication of a biased water flux across the membrane in either direction. The total amount of water efflux and influx are always almost the same as in all of the studied transporters (Figs. 1–3). This observation, which is expected given the absence of an osmotic gradient or hydrostatic pressure difference across the simulated membrane, also supports a completely passive mode of water transport in membrane transporters.

Universality of Water-Conducting States in Transporters. One of the unique aspects of the present study is the demonstration of water-conducting states in diverse families and distinct functional states of membrane transporters: vSGLT and Mhp1 represent, respectively, a substrate-bound IF state and an OF state of LeuT-fold transporters; Glt_{ph} and GlpT represent, respectively, an intermediate state of an SLC1 and an IF state of an MFS transporter; and maltose transporter is an OF state of ABC transporters. The simulations describe the phenomenon not only for several experimentally demonstrated cases (6–9, 22, 30, 35, 36) but also for a number of additional transporters.

Although the formation of water-conducting states in vSGLT is mediated by mostly localized structural fluctuations, for the remainder of the studied transporters, the phenomenon appears to be correlated with more global structural changes, which are necessary for cycling through major functional states. This observation is in line with the notion that water-conducting states may generally arise as short-lived intermediates every time the protein undergoes a transition from one major state to another (Fig. 4).

Membrane transporters face an extremely challenging task to function effectively: a transporter needs to achieve highly coordinated gating motions at the cytoplasmic and extracellular gates, which are often spatially far from each other. Only a perfect coordination of the two gates can ensure the formation of a truly occluded state that would prevent even the leak of small species such as water. Given the soft mechanical properties of transporter proteins, it comes as no surprise to observe harmless imperfections in the overall gating motions, which manifest themselves in the formation of water-conducting states. It would, of course, be a concern if these channels were large enough to leak the substrate, and/or long-lived to allow very large amounts of smaller species to permeate across the membrane. Neither of

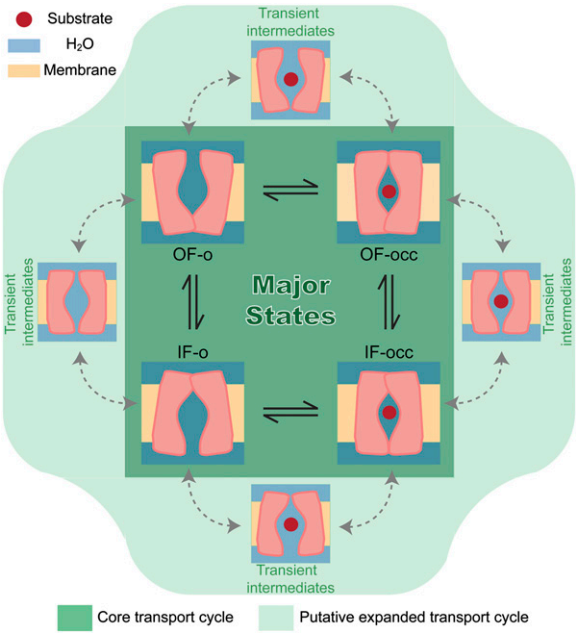

Fig. 4. Formation of water-conducting states during the transport cycle. The core transport cycle of a membrane transporter (dark green region) relies on interconversion of the protein structure between major known functional states—namely, outward-facing open (OF-o), outward-facing occluded (OF-occ), inward-facing open (IF-o), and inward-facing occluded (IF-occ) states, which have been observed in various crystal structures (24, 34, 40, 41, 45). An expanded view of the transport cycle (light green area) would involve a number of additional intermediates that arise during the transition between the major states, which due to their transient nature have not yet been structurally characterized by experiments, but can account for the uncoupled water and ion transport during the transport cycle.

these aspects appears to be the observed in our results, because the leaky states are only large enough for small species such as water. Furthermore, it appears that these states only transiently rise during the transport cycle, an attribute that might make them difficult to capture experimentally. Viewing the formation of these leaky states as a consequence of deviation of a transporter protein from a perfect, machine-like behavior, it is not surprising that such mechanical defects might not necessarily arise during each and every large-scale transition of every transporter. In fact, in several other transporter systems studied in our laboratory by comparably long simulations, we did not observe the formation of such water-conducting states. Furthermore, several experimental studies have also illustrated the occurrence of water and ion leak only for specific states of the studied transporters (6, 8, 20, 50). Depending on the protein architecture, degree of conformational changes involved in the cycle, and even the nature of the substrate, some transporters and some transitions might be more prone to the formation of water-conducting states.

Materials and Methods

A summary of the studied transporters is provided in Table 1. All of the transporter proteins were simulated in the explicit presence of membrane, water, and ions. Simulations were performed using NAMD 2.6 (51) or Desmond on Anton (52), using the CHARMM force field (53) for proteins, lipids, ions, and substrates, and TIP3P model for explicit water (54). After the initial minimization and equilibration, the systems were subjected to production simulations in the constant pressure and constant temperature (NPT) ensemble (Table 1; see *SI Materials and Methods* for more detail).

ACKNOWLEDGMENTS. Simulations in this study have been performed using National Science Foundation's Extreme Science and Engineering Discovery Environment (XSEDE) Resources Grant MCA06N060 and Anton at Pittsburg Supercomputing Center Grant MCB100017P. Support was also provided by National Institutes of Health Grants R01-GM086749, U54-GM087519, and P41-GM104601.

1. DeFelice LJ (2004) Transporter structure and mechanism. *Trends Neurosci* 27(6): 352–359.
2. Jardetzky O (1966) Simple allosteric model for membrane pumps. *Nature* 211(5052): 969–970.
3. Forrest LR, Krämer R, Ziegler C (2011) The structural basis of secondary active transport mechanisms. *Biochim Biophys Acta* 1807(2):167–188.
4. Oldham ML, Davidson AL, Chen J (2008) Structural insights into ABC transporter mechanism. *Curr Opin Struct Biol* 18(6):726–733.
5. Gadsby DC (2009) Ion channels versus ion pumps: The principal difference, in principle. *Nat Rev Mol Cell Biol* 10(5):344–352.
6. Zeuthen T (2010) Water-transporting proteins. *J Membr Biol* 234(2):57–73.
7. DeFelice LJ, Goswami T (2007) Transporters as channels. *Annu Rev Physiol* 69:87–112.
8. Andrini O, Ghezzi C, Murer H, Forster IC (2008) The leak mode of type II $Na(^+)$-$P(_i)$ cotransporters. *Channels (Austin)* 2(5):346–357.
9. Loo DD, et al. (1999) Passive water and ion transport by cotransporters. *J Physiol* 518(Pt 1):195–202.
10. Zeuthen T, Stein WD (1994) Cotransport of salt and water in membrane proteins: Membrane proteins as osmotic engines. *J Membr Biol* 137(3):179–195.
11. Meinild A, Klaerke DA, Loo DD, Wright EM, Zeuthen T (1998) The human Na^+-glucose cotransporter is a molecular water pump. *J Physiol* 508(Pt 1):15–21.
12. Zeuthen T, Belhage B, Zeuthen E (2006) Water transport by Na^+-coupled cotransporters of glucose (SGLT1) and of iodide (NIS). The dependence of substrate size studied at high resolution. *J Physiol* 570(Pt 3):485–499.
13. Duquette PP, Bissonnette P, Lapointe JY (2001) Local osmotic gradients drive the water flux associated with $Na(^+)$/glucose cotransport. *Proc Natl Acad Sci USA* 98(7):3796–3801.
14. Gagnon MP, Bissonnette P, Deslandes LM, Wallendorff B, Lapointe JY (2004) Glucose accumulation can account for the initial water flux triggered by Na^+/glucose cotransport. *Biophys J* 86(1 Pt 1):125–133.
15. Naftalin RJ (2008) Osmotic water transport with glucose in GLUT2 and SGLT. *Biophys J* 94(10):3912–3923.
16. Khalili-Araghi F, et al. (2009) Molecular dynamics simulations of membrane channels and transporters. *Curr Opin Struct Biol* 19(2):128–137.
17. Loo DD, Zeuthen T, Chandy G, Wright EM (1996) Cotransport of water by the Na^+/glucose cotransporter. *Proc Natl Acad Sci USA* 93(23):13367–13370.
18. Zeuthen T, Zeuthen E, Klaerke DA (2002) Mobility of ions, sugar, and water in the cytoplasm of *Xenopus* oocytes expressing $Na(^+)$-coupled sugar transporters (SGLT1). *J Physiol* 542(Pt 1):71–87.
19. Choe S, Rosenberg JM, Abramson J, Wright EM, Grabe M (2010) Water permeation through the sodium-dependent galactose cotransporter vSGLT. *Biophys J* 99(7):L56–L58.
20. Sasseville LJ, Cuervo JE, Lapointe JY, Noskov SY (2011) The structural pathway for water permeation through sodium-glucose cotransporters. *Biophys J* 101(8):1887–1895.
21. Hamann S, Kiilgaard JF, la Cour M, Prause JU, Zeuthen T (2003) Cotransport of H^+, lactate, and H_2O in porcine retinal pigment epithelial cells. *Exp Eye Res* 76(4):493–504.
22. Santacroce M, Castagna M, Sacchi VF (2010) Passive water permeability of some wild type and mutagenized amino acid cotransporters of the SLC6/NSS family expressed in *Xenopus laevis* oocytes. *Comp Biochem Physiol A Mol Integr Physiol* 156(4):509–517.
23. MacAulay N, Zeuthen T, Gether U (2002) Conformational basis for the $Li(^+)$-induced leak current in the rat gamma-aminobutyric acid (GABA) transporter-1. *J Physiol* 544(Pt 2):447–458.
24. Faham S, et al. (2008) The crystal structure of a sodium galactose transporter reveals mechanistic insights into Na^+/sugar symport. *Science* 321(5890):810–814.
25. Zampighi GA, et al. (1995) A method for determining the unitary functional capacity of cloned channels and transporters expressed in *Xenopus laevis* oocytes. *J Membr Biol* 148(1):65–78.
26. Boudker O, Ryan RM, Yernool D, Shimamoto K, Gouaux E (2007) Coupling substrate and ion binding to extracellular gate of a sodium-dependent aspartate transporter. *Nature* 445(7126):387–393.
27. Reyes N, Ginter C, Boudker O (2009) Transport mechanism of a bacterial homologue of glutamate transporters. *Nature* 462(7275):880–885.
28. Verdon G, Boudker O (2012) Crystal structure of an asymmetric trimer of a bacterial glutamate transporter homolog. *Nat Struct Mol Biol* 19(3):355–357.
29. MacAulay N, Gether U, Klaerke DA, Zeuthen T (2001) Water transport by the human Na+-coupled glutamate cotransporter expressed in *Xenopus* oocytes. *J Physiol* 530(Pt 3):367–378.
30. MacAulay N, Gether U, Klaeke DA, Zeuthen T (2002) Passive water and urea permeability of a human $Na(^+)$-glutamate cotransporter expressed in *Xenopus* oocytes. *J Physiol* 542(Pt 3):817–828.
31. Vandenberg RJ, Handford CA, Campbell EM, Ryan RM, Yool AJ (2011) Water and urea permeation pathways of the human excitatory amino acid transporter EAAT1. *Biochem J* 439(2):333–340.
32. Huang Z, Tajkhorshid E (2008) Dynamics of the extracellular gate and ion-substrate coupling in the glutamate transporter. *Biophys J* 95(5):2292–2300.
33. Huang Z, Tajkhorshid E (2010) Identification of the third Na^+ site and the sequence of extracellular binding events in the glutamate transporter. *Biophys J* 99(5):1416–1425.
34. Huang Y, Lemieux MJ, Song J, Auer M, Wang DN (2003) Structure and mechanism of the glycerol-3-phosphate transporter from *Escherichia coli*. *Science* 301(5633):616–620.
35. Fischbarg J, et al. (1990) Glucose transporters serve as water channels. *Proc Natl Acad Sci USA* 87(8):3244–3247.
36. Zeuthen T, Zeuthen E, Macaulay N (2007) Water transport by GLUT2 expressed in *Xenopus* laevis oocytes. *J Physiol* 579(Pt 2):345–361.
37. Enkavi G, Tajkhorshid E (2010) Simulation of spontaneous substrate binding revealing the binding pathway and mechanism and initial conformational response of GlpT. *Biochemistry* 49(6):1105–1114.
38. Law CJ, Enkavi G, Wang DN, Tajkhorshid E (2009) Structural basis of substrate selectivity in the glycerol-3-phosphate: Phosphate antiporter GlpT. *Biophys J* 97(5): 1346–1353.
39. Pantazopoulou A, Diallinas G (2007) Fungal nucleobase transporters. *FEMS Microbiol Rev* 31(6):657–675.
40. Weyand S, et al. (2008) Structure and molecular mechanism of a nucleobase-cation-symport-1 family transporter. *Science* 322(5902):709–713.
41. Shimamura T, et al. (2010) Molecular basis of alternating access membrane transport by the sodium-hydantoin transporter Mhp1. *Science* 328(5977):470–473.
42. Zhao Y, et al. (2011) Substrate-modulated gating dynamics in a Na^+-coupled neurotransmitter transporter homologue. *Nature* 474(7349):109–113.
43. Claxton DP, et al. (2010) Ion/substrate-dependent conformational dynamics of a bacterial homolog of neurotransmitter:sodium symporters. *Nat Struct Mol Biol* 17(7): 822–829.
44. Bordignon E, Grote M, Schneider E (2010) The maltose ATP-binding cassette transporter in the 21st century—towards a structural dynamic perspective on its mode of action. *Mol Microbiol* 77(6):1354–1366.
45. Oldham ML, Khare D, Quiocho FA, Davidson AL, Chen J (2007) Crystal structure of a catalytic intermediate of the maltose transporter. *Nature* 450(7169):515–521.
46. Newstead S, et al. (2009) Insights into how nucleotide-binding domains power ABC transport. *Structure* 17(9):1213–1222.
47. Wen PC, Tajkhorshid E (2011) Conformational coupling of the nucleotide-binding and the transmembrane domains in ABC transporters. *Biophys J* 101(3):680–690.
48. Singh SK, Yamashita A, Gouaux E (2007) Antidepressant binding site in a bacterial homologue of neurotransmitter transporters. *Nature* 448(7156):952–956.
49. Perez C, Koshy C, Yildiz O, Ziegler C (2012) Alternating-access mechanism in conformationally asymmetric trimers of the betaine transporter BetP. *Nature* 490(7418): 126–130.
50. Schicker K, et al. (2012) Unifying concept of serotonin transporter-associated currents. *J Biol Chem* 287(1):438–445.
51. Phillips JC, et al. (2005) Scalable molecular dynamics with NAMD. *J Comput Chem* 26(16):1781–1802.
52. Shaw DE, et al. (2009) Millisecond-scale molecular dynamics simulations on Anton. *SC '09: Proceedings of the Conference on High Performance Computing Networking, Storage and Analysis* (Assoc for Computing Machinery, Portland, OR), pp 39:1–39:11.
53. MacKerell AD, Jr., et al. (1998) All-atom empirical potential for molecular modeling and dynamics studies of proteins. *J Phys Chem B* 102:3586–3616.
54. Jorgensen WL, Chandrasekhar J, Madura JD, Impey RW, Klein ML (1983) Comparison of simple potential functions for simulating liquid water. *J Chem Phys* 79:926–935.